

# SUSY-QCD corrections in the squark–gluino sector

W. Beenakker<sup>a,\*†</sup> and R. Höpker<sup>b</sup>

<sup>a</sup>Instituut–Lorentz, University of Leiden, P.O. Box 9506, NL–2300 RA Leiden, The Netherlands.

<sup>b</sup>DESY, Theory Division, Notkestrasse 85, D–22603 Hamburg, Germany.

A status report is given of the calculations of next-to-leading-order ( $N = 1$ ) supersymmetric QCD corrections to the production of squarks and gluinos in  $p\bar{p}/pp$  collisions. The implementation of these SUSY-QCD corrections leads to more stable theoretical predictions and to a substantial increase of the production cross-sections. In addition we give a discussion of the use of the  $\overline{MS}$  scheme for renormalizing the coupling constants in the QCD sector of ( $N = 1$ ) supersymmetric theories.

## 1. INTRODUCTION

The colored squarks ( $\tilde{q}_L, \tilde{q}_R$ ) and gluinos ( $\tilde{g}$ ), the supersymmetric partners of the quarks ( $q$ ) and gluons ( $g$ ), can be searched for most efficiently at high-energy hadron colliders. As R-parity is conserved in the QCD sector of ( $N = 1$ ) supersymmetric theories, these particles are always produced in pairs. At the moment they can be searched for at the Fermilab Tevatron, a  $p\bar{p}$  collider with a centre-of-mass energy of 1.8 TeV. In the future the CERN Large Hadron Collider (LHC), a  $pp$  collider with an envisaged centre-of-mass energy of 14 TeV, will allow to cover mass values up to 1–2 TeV.

At present the main search strategy employed at the Tevatron involves the search for jets and missing transverse energy [1,2]. R-parity conserving decay cascades of the squarks and gluinos result in Standard-Model hadrons, i.e., jets, and LSP's ( $\chi_1^0$ ), responsible for the missing energy. An example of a complete process, involving production and subsequent decay, is given by

$$p\bar{p} \rightarrow \tilde{q}_L + \tilde{q}_R \rightarrow \chi^+ q' + \chi_1^0 \bar{q} \rightarrow \chi_1^0 q \bar{q}' q' + \chi_1^0 \bar{q},$$

with  $q'$  the isospin partner of  $q$ . The present status of the squark and gluino searches, based on this strategy, is depicted in Fig. 1. As the search has been negative up to now, only lower bounds on the squark and gluino masses are given. The

\*Partially supported by EU contract CHRX-CT-92-0004.

†Research supported by a fellowship of the Royal Dutch Academy of Arts and Sciences.

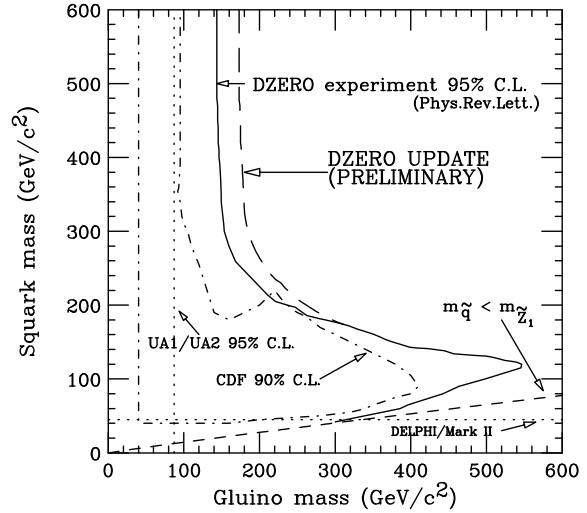


Figure 1. Experimental lower mass bounds for squarks ( $\tilde{q} \neq \tilde{t}$ ) and gluinos from the Tevatron [2].

present lower mass bounds, derived from Fig. 1, are ( $\tilde{q} \neq \tilde{t}$ )

$$m_{\tilde{g}} \geq 175 \text{ GeV},$$

$$m_{\tilde{q}} \geq 175 \text{ GeV} \quad \text{for} \quad m_{\tilde{g}} \leq 300 \text{ GeV}.$$

So far this analysis has been based on the lowest-order (LO) production cross-sections. For obtaining adequate theoretical predictions the LO cross-sections are in general not sufficient. The most important arguments in favor of an analysis

that takes into account the next-to-leading-order (NLO) SUSY-QCD corrections are:

- The LO cross-sections have a strong dependence on the *a priori* unknown renormalization scale  $Q_R$ . Consequently, the theoretical predictions have in general an uncertainty that is almost as large as the cross-section itself. By implementing the NLO corrections a substantial reduction of the scale dependence is expected.
- From experience with similar processes (e.g. hadroproduction of top quarks), the NLO QCD corrections are expected to be of the order of +30%.
- An enhancement of the cross-section would lead to a higher value for the lower mass bounds for squarks and gluinos.
- In case of discovery of squarks and gluinos, a precise knowledge of the total cross-sections is required for the determination of the masses of the particles. In contrast to the production of e.g. top-quark or Z-boson pairs, it seems unlikely that the masses of squarks and gluinos can be determined by means of reconstruction (in view of the invisible LSP's). Probably they can only be inferred from the experimental production rates and the theoretical prediction for the total cross-section.

Here we report on the status of the calculations of NLO SUSY-QCD corrections to the production of (on-shell) squarks and gluinos in  $p\bar{p}/pp$  collisions, based on the studies presented in [3]. For a more comprehensive report on this topic we refer to [4].

## 2. TECHNICAL SET-UP

We consider the following hadronic production processes (generically depicted in Fig. 2):

$$p\bar{p}/pp \rightarrow \tilde{q}\tilde{\bar{q}}, \tilde{q}\tilde{q}, \tilde{g}\tilde{g}, \tilde{q}\tilde{\bar{g}} \quad (\tilde{q} \neq \tilde{t}), \quad (1)$$

where the chiralities and flavors of the squarks (e.g.  $\tilde{u}_L, \tilde{d}_R$ ) as well as the charge-conjugate final states (e.g.  $\tilde{\bar{q}}\tilde{q}$ ) are implicitly summed over.

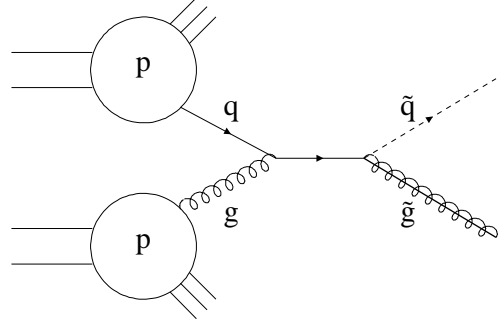


Figure 2. Generic Feynman diagram for the production of squarks and gluinos in  $p\bar{p}/pp$  collisions.

In analogy to the experimental analysis, we exclude top-squarks from the final state and take all produced squarks to be mass degenerate. A study of the production of pairs of top-squarks is in progress, including the (model-dependent) mixing effects in the squark sector. At the partonic level (right-hand side of Fig. 2) many different subprocesses contribute at LO and NLO, corresponding to different flavors/chiralities of the squarks and different initial-state partons. The initial-state partons are made up of the massless gluons and the five light quark flavors ( $n_f = 5$ ), which are considered to be massless as well. Note that not all initial states are possible for a given final state. At LO, for instance, the production of squark–antisquark final states requires quark–antiquark or gluon–gluon initial states, whereas the squark–gluino final states are only possible in quark–gluon reactions.

The NLO SUSY-QCD corrections comprise the virtual corrections (consisting of self-energy corrections, vertex corrections, and box diagrams), real-gluon radiation (with an additional gluon attached to the LO diagrams), and the radiation of a massless quark (opening additional initial-state channels: e.g.  $gq \rightarrow \tilde{q}\tilde{\bar{q}}q$ ).

For the particles inside the loops we use the complete supersymmetric QCD spectrum, i.e., gluons, gluinos, all quarks, and all squarks. We have excluded the top-squarks from the final states. In order to have a consistent NLO calcula-

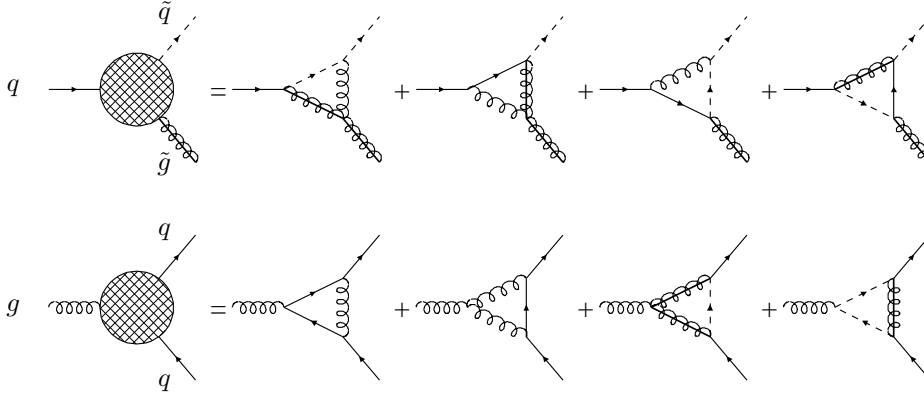


Figure 3. Feynman diagrams for the virtual NLO SUSY-QCD corrections to the quark-squark-gluino vertex (Yukawa coupling) and the quark-quark-gluon vertex (gauge coupling).

tion, however, we have to take these top-squarks into account inside loops. For the sake of simplicity we take them to be mass-degenerate with the other squarks. For the top quark we use the mass  $m_t = 175$  GeV. Consequently the final results will depend on two free parameters: the squark mass  $m_{\tilde{q}}$  and the gluino mass  $m_{\tilde{g}}$ .

For the internal gluon propagators we use the Feynman gauge. As a result, Faddeev-Popov ghost contributions have to be taken into account in the gluon self-energy and the three-gluon vertex corrections. For the external gluon lines only the transverse polarizations are needed.

The divergences appearing in the NLO corrections are regularized by performing the calculations in  $n = 4 - 2\varepsilon$  dimensions. These divergences consist of ultraviolet (UV), infra-red (IR), and collinear divergences, and show up as poles of the form  $\varepsilon^{-i}$  ( $i = 1, 2$ ). For the treatment of the  $\gamma_5$  Dirac matrix, entering through the quark-squark-gluino Yukawa couplings, we use the ‘naive’ scheme. This involves a  $\gamma_5$  that anti-commutes with the other gamma matrices. This is a legitimate scheme at the one-loop level for anomaly-free theories.

The UV divergences can be removed by renormalizing the coupling constants and the masses of the massive particles. In the case of the mass renormalization we have opted for an on-shell scheme with real subtraction point, involving the subtraction of the real part of the on-shell self-

energies at the real-valued pole masses. For the renormalization of the QCD coupling constant one usually resorts to the modified Minimal Subtraction ( $\overline{MS}$ ) scheme. The  $\overline{MS}$  scheme involves  $n$ -dimensional regularization, i.e., treating fields, phase space, and loop momenta in  $n$  dimensions. The UV  $1/\varepsilon$  poles are subtracted, together with specific transcendental constants, at an *a priori* arbitrary subtraction point (renormalization scale)  $Q_R$ . In supersymmetric theories, however, a complication occurs. In  $n \neq 4$  dimensions the  $\overline{MS}$  scheme introduces a mismatch between the number of gluon ( $n - 2$ ) and gluino (2) degrees of freedom. As these  $\mathcal{O}(\varepsilon)$  mismatches will result in finite contributions, the  $\overline{MS}$  scheme violates supersymmetry explicitly. In particular, the  $q\tilde{q}\tilde{g}$  Yukawa coupling  $\hat{g}_s$ , which by supersymmetry should coincide with the  $qqg$  gauge coupling  $g_s$ , deviates from  $g_s$  by a finite amount at the one-loop order. Requiring the physical amplitudes to be independent of the renormalization scheme, a shift between the bare Yukawa and gauge couplings must be introduced in the  $\overline{MS}$  scheme,

$$\hat{g}_s = g_s \left[ 1 + \frac{\alpha_s}{4\pi} \left( \frac{2}{3}N - \frac{1}{2}C_F \right) \right] = g_s \left[ 1 + \frac{\alpha_s}{3\pi} \right], \quad (2)$$

which effectively subtracts the contributions of the false, non-supersymmetric degrees of freedom (also called  $\varepsilon$  scalars) [5]. Here we used  $\alpha_s = g_s^2/(4\pi)$ ,  $N = 3$ , and  $C_F = (N^2 - 1)/(2N) = 4/3$ .

The need for introducing a finite shift is best demonstrated for the effective (one-loop corrected) Yukawa coupling (see Fig. 3), which must

be equal to the effective gauge coupling in an exact supersymmetric world with massless gluons/gluinos and equal-mass quarks/squarks. For the sake of simplicity we define the one-loop corrected effective couplings  $\Gamma_s^{\text{eff}}(Q^2) = g_s [1 + \delta(Q^2)]$  and  $\hat{\Gamma}_s^{\text{eff}}(Q^2) = \hat{g}_s [1 + \hat{\delta}(Q^2)]$  in the limit of on-shell quarks/squarks and almost on-shell gluons/gluinos, with virtuality  $Q^2 \ll m_{\tilde{q}}^2 = m_q^2$ . In this limit the couplings do not contain gauge-dependent terms. In the  $\overline{MS}$  scheme we find after charge renormalization [6]

$$\overline{MS}: \frac{\hat{\Gamma}_s^{\text{eff}}(Q^2)}{\hat{g}_s} = \frac{\Gamma_s^{\text{eff}}(Q^2)}{g_s} + \frac{\alpha_s}{4\pi} \left( \frac{1}{2} C_F - \frac{2}{3} N \right). \quad (3)$$

The difference between the two effective couplings coincides with the shift (2). Taking into account this finite shift of the bare couplings in the  $\overline{MS}$  scheme, both effective couplings become identical at the one-loop level. In this way supersymmetry is preserved and the  $\overline{MS}$  scheme becomes a workable one.

An alternative renormalization scheme is the modified Dimensional Reduction ( $\overline{DR}$ ) scheme. This scheme consists in treating the fields in 4 dimensions and the phase space and loop momenta in  $n$  dimensions. As such no mismatch is introduced and supersymmetry is preserved. At the level of the above-defined effective couplings this is reflected in the equality [6]

$$\overline{DR}: \frac{\hat{\Gamma}_s^{\text{eff}}(Q^2)}{\hat{g}_s} = \frac{\Gamma_s^{\text{eff}}(Q^2)}{g_s}. \quad (4)$$

As a result, both couplings are identical order by order. It should be noted that the transition from the effective gauge coupling in  $\overline{MS}$  to the one in  $\overline{DR}$  involves a well-known finite renormalization  $(\alpha_s N)/(24\pi) = \alpha_s/(8\pi)$ .

In the following we use the  $\overline{MS}$  renormalization scheme in combination with the finite shift of the Yukawa coupling. In this way supersymmetry is preserved on the one hand, while on the other hand the definition of the strong gauge coupling corresponds to the usual Standard-Model measurements. In addition to the poles also some logarithms are subtracted in order to decouple the massive particles (top quarks, squarks, gluinos) from the running of  $\alpha_s(Q_R^2)$ . The  $Q_R^2$  evolution of the strong coupling is in this decoupling renormalization scheme completely determined by the light-particle spectrum (gluons and  $n_f = 5$  mass-

less quarks):

$$\frac{\partial g_s^2(Q_R^2)}{\partial \log(Q_R^2)} = -\alpha_s^2(Q_R^2) \left[ \frac{11}{3} N - \frac{2}{3} n_f \right]. \quad (5)$$

The above described methods to renormalize the UV divergences result in cross-sections that are UV finite. Nevertheless there are still divergences left. The IR ones will cancel in the sum of virtual corrections and soft-gluon radiation. In order to separate soft from hard radiation a cut-off  $\Delta$  is introduced in the invariant mass corresponding to the radiated gluon and one of the produced massive particles. If soft and hard contributions are added up, any  $\Delta$  dependence disappears from the cross-sections for  $\Delta \rightarrow 0$ . The remaining collinear singularities, finally, can be absorbed into the renormalization of the parton densities, carried out in the  $\overline{MS}$  mass-factorization scheme. This introduces yet another *a priori* unknown scale, the factorization scale  $Q_F$ .

In the context of mass factorization an interesting observation was made during the comparison of the  $\overline{MS}$  and  $\overline{DR}$  results. Even after correcting for  $\varepsilon$ -scalar contributions, leading to finite differences between the splitting functions in  $\overline{MS}$  and  $\overline{DR}$  [7], discrepancies of  $\mathcal{O}(m_{\tilde{q}}^2, m_q^2)$  persisted. The exact source of these discrepancies is under investigation. This phenomenon is, however, not an artefact of supersymmetry, since it is also observed in the (pure QCD) process of top-quark production [8].

The last singularity we have to deal with is of kinematical nature. If the gluinos are lighter than the squarks, on-shell squarks can decay into massless quarks plus gluinos ( $\tilde{q} \rightarrow q\tilde{g}$ ). This means that inside the phase space of massless-quark-radiation processes like  $g\tilde{q} \rightarrow \tilde{g}\tilde{g}\tilde{q}$  (see Fig. 4) explicit particle poles can emerge. These particle poles, however, correspond to on-shell (LO) production of the intermediate on-shell squark state, with subsequent (LO) decay into a massless quark plus gluino. In our narrow-width approach, consisting in neglecting the finite decay widths of the squarks/gluinos whenever possible, these situations are already accounted for by the LO cross-sections (e.g. squark-gluino production in Fig. 4). In order to avoid double counting these kinematical situations have to be subtracted from

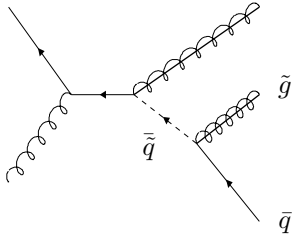


Figure 4. Example of a NLO Feynman diagram that can give rise to an on-shell intermediate squark state.

the NLO corrections. Similar subtractions have to be performed if the squarks are lighter than the gluinos. For more details concerning the exact subtraction procedure we refer to [4].

### 3. RESULTS

At the partonic level at least three sources of large corrections can be identified. Indicating the velocity of the produced heavy particles in their centre-of-mass system by  $\beta$ , two of these sources reside in the region near threshold ( $\beta \ll 1$ ), from which an important part of the contributions to the hadronic cross-sections originates. First of all, the exchange of (long-range) Coulomb gluons between the slowly moving massive particles in the final state (see first generic diagram of Fig. 5) leads to a singular correction factor  $\sim \pi\alpha_s/\beta$ , which compensates the LO phase-space suppression factor  $\beta$ . It should be noted, however, that the finite lifetimes of the squarks/gluinos reduce (screen) this effect considerably. Secondly, as a result of the strong energy dependence of the

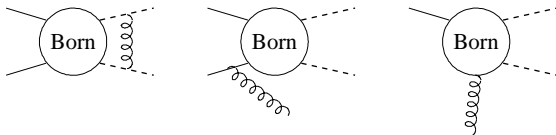


Figure 5. Generic diagrams leading to the Coulomb singularity, the large threshold logarithms, and the high-energy plateau, respectively.

cross-sections near threshold, large “soft” corrections  $\sim \log^i(\beta^2)$  ( $i = 1, 2$ ) are observed in the initial-state gluon-radiation contribution (see second generic diagram of Fig. 5). At high energies, finally, the NLO partonic cross-sections behave asymptotically as a constant, rather than scaling with  $1/s$  like the LO cross-sections. This is caused by the presence of almost on-shell IR gluons in space-like propagators, as appearing in the contributions from hard-gluon/quark radiation (see third generic diagram of Fig. 5). All these effects can be calculated analytically in NLO, providing powerful checks on the partonic results [3,4].

After convolution of the partonic cross-sections with the relevant parton densities, the hadronic cross-sections are obtained. When discussing LO and NLO results, we calculate all quantities [ $\alpha_s(Q_R^2)$ , the parton densities, and the partonic cross-sections] in LO and NLO, respectively. Bearing this in mind the hadronic results can be summarized as follows.

(i) As is exemplified in Fig. 6, we find that the theoretical predictions for the production cross-sections are stabilized considerably by taking into account the NLO SUSY-QCD corrections. In all processes, for both the Tevatron and the LHC, it is observed that the dependence on the renormalization/factorization scale  $Q$  ( $Q = Q_R = Q_F$ ) is quite steep and monotonic in LO, whereas the  $Q$  dependence is reduced by roughly a factor of 2.5–4 in NLO for reasonable variations of the scale. Even a broad maximum develops for scales that are roughly a factor of 3–4 smaller than the average mass of the final-state particles. The variation of the cross-sections as a result of different NLO parametrizations of the parton densities is  $\lesssim 10\%$  at the Tevatron and  $\lesssim 13\%$  at the LHC, where the gluon densities are more important. It should, however, be noted that considering such a sample of different parton densities could lead to an underestimation of the actual theoretical uncertainties.

(ii) From now on we use GRV94 parton densities and conservatively take as default scale  $Q$  the average mass of the produced particles. The K-factors,  $K = \sigma_{NLO}/\sigma_{LO}$ , depend strongly on the process. This is exemplified in Fig. 7 for the Tevatron. For both collider types the NLO cor-

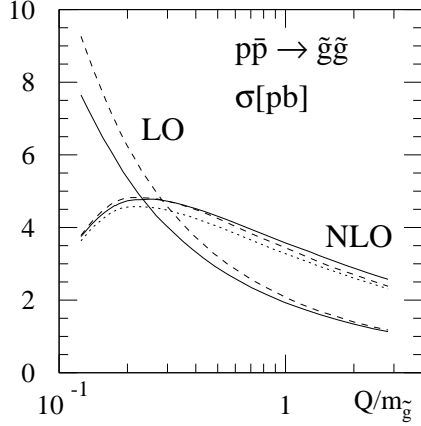


Figure 6. The scale and parton-density dependence of the LO and NLO cross-sections for gluino-pair production at the Tevatron. Parton densities: GRV94 (solid), CTEQ3 (dashed), and MRSA' (dotted). Mass parameters:  $m_{\tilde{q}} = 280$  GeV,  $m_{\tilde{g}} = 200$  GeV, and  $m_t = 175$  GeV.

rections are positive and large (up to +90%) for the dominant production cross-sections, involving at least one gluino in the final state. The corresponding K-factors also exhibit a sizeable dependence on the squark and gluino masses (especially the  $m_{\tilde{g}}$  dependence of  $K_{\tilde{g}\tilde{g}}$  is large). The NLO corrections for squark final states are moderate ( $\lesssim +30\%$ ). In view of the direct link between the total cross-sections and the experimental determination of the squark/gluino masses in case of discovery, the inclusion of the NLO SUSY-QCD corrections is indispensable.

(iii) Comparison of the NLO cross-sections with the cross-sections used in the Tevatron analysis (LO, EHLQ parton densities, and a scale  $Q$  that equals the partonic centre-of-mass energy [1,2]) reveals that the NLO corrections raise the lower mass bounds for squarks and gluinos by +10 GeV to +30 GeV.

(iv) Apart from the total cross-sections, also distributions with respect to the rapidity ( $y$ ) and transverse momentum ( $p_t$ ) of one of the outgoing massive particles can be studied. The K-factors for these distributions are independent of  $y$  for

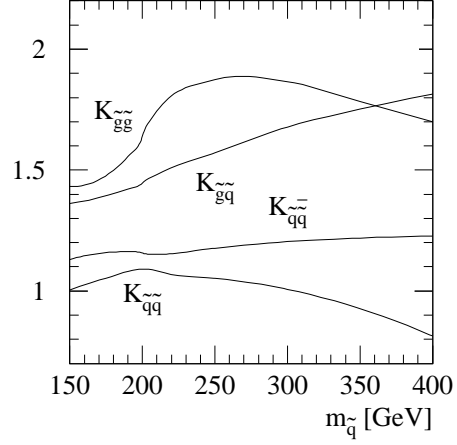


Figure 7. The K-factors for the Tevatron. Parton densities: GRV94 with  $Q = \text{average mass}$ . Mass parameters:  $m_{\tilde{g}} = 200$  GeV and  $m_t = 175$  GeV.

all practical purposes and hardly depend on  $p_t$ , except for large values of  $p_t$  where the NLO corrections make the distributions somewhat softer. Consequently, multiplication of the LO distributions with the above-defined K-factors for the total cross-sections approximates the full NLO results quite well.

## REFERENCES

1. F. Abe *et al.*, CDF Coll., *Phys. Rev. Lett.* **75** (1995) 613.
2. S. Abachi *et al.*, D0 Coll., *Phys. Rev. Lett.* **75** (1995) 618.
3. W. Beenakker, R. Höpker, M. Spira and P.M. Zerwas, *Phys. Rev. Lett.* **74** (1995) 2905; *Z. Phys.* **C69** (1995) 163.
4. W. Beenakker, R. Höpker, M. Spira and P.M. Zerwas, *DESY-Report* in preparation.
5. S.P. Martin and M.T. Vaughn, *Phys. Lett.* **B318** (1993) 331.
6. W. Beenakker, R. Höpker and P.M. Zerwas, *DESY-Report* 96-022, *hep-ph/9602378*.
7. J.G. Körner and M. Tung, *Z. Phys.* **C64** (1994) 255.
8. W. Beenakker, H. Kuijf, W.L. van Neerven and J. Smith, *Phys. Rev.* **D40** (1989) 54.